ESC European Society of Cardiology

Cardiovascular Research (2017) **113**, 1603–1614
doi:10.1093/cvr/cvx132

MicroRNA-532 protects the heart in acute myocardial infarction, and represses prss23, a positive regulator of endothelial-to-mesenchymal transition

Ahmed S. Bayoumi[1], Jian-Peng Teoh[1], Tatsuya Aonuma[1], Zhize Yuan[1], Xiaofen Ruan[1], Yaoliang Tang[1,2], Huabo Su[1,3], Neal L. Weintraub[1,2], and Il-Man Kim[1,4]*

[1]Vascular Biology Center; [2]Department of Medicine; [3]Department of Pharmacology and Toxicology; and [4]Department of Biochemistry and Molecular Biology, Medical College of Georgia, Augusta University, CB-3717, 1459 Laney Walker Blvd, Augusta, GA 30912, USA

Received 29 November 2016; revised 10 May 2017; editorial decision 20 June 2017; accepted 7 July 2017; online publish-ahead-of-print 11 July 2017

Time for primary review: 44 days

Aims Acute myocardial infarction (MI) leads to cardiac remodelling and development of heart failure. Insufficient myocardial capillary density after MI is considered a critical determinant of this process. MicroRNAs (miRs), negative regulators of gene expression, have emerged as important players in MI. We previously showed that miR-532-5p (miR-532) is up-regulated by the β-arrestin-biased β-adrenergic receptor antagonist (β-blocker) carvedilol, which activates protective pathways in the heart independent of G protein-mediated second messenger signalling. Here, we hypothesize that β_2-adrenergic receptor/β-arrestin-responsive miR-532 confers cardioprotection against MI.

Methods and results Using cultured cardiac endothelial cell (CEC) and *in vivo* approaches, we show that CECs lacking miR-532 exhibit increased transition to a fibroblast-like phenotype via endothelial-to-mesenchymal transition (EndMT), while CECs over-expressing miR-532 display decreased EndMT. We also demonstrate that knockdown of miR-532 in mice causes abnormalities in cardiac structure and function as well as reduces CEC proliferation and cardiac vascularization after MI. Mechanistically, cardioprotection elicited by miR-532 is in part attributed to direct repression of a positive regulator of maladaptive EndMT, prss23 (a protease serine 23) in CECs.

Conclusions In conclusion, these findings reveal a pivotal role for miR-532-prss23 axis in regulating CEC function after MI, and this novel axis could be suitable for therapeutic intervention in ischemic heart disease.

Keywords β-Arrestin • Biased G protein-coupled receptor signalling • Cardioprotection • Endothelial-to-mesenchymal transition • MicroRNAs

1. Introduction

Myocardial infarction (MI) results from insufficient blood supply to the heart and causes substantial death of cardiac cells and scar formation.[1,2] Cardiac tissue hypoxia in the setting of MI triggers endothelial-to-mesenchymal transition (EndMT), which further contributes to cardiac dysfunction by increasing cardiac fibroblastic content and limiting cardiac vasculature.[3] MI is also associated with reduced myocardial capillary flow reserve and capillary density, resulting in impaired tissue perfusion as well as augmented cellular injury and scar formation.[4,5]

Cardiac injury is accompanied by dynamic changes in the expression of microRNAs (miRNAs or miRs), which are endogenous, small single strand, non-coding RNAs that down-regulate target genes.[6,7] MiRs are increasingly recognized as important regulators of cardiac function and disease.[8,9] The β-adrenergic receptor antagonist (β-blocker) carvedilol (Carv) promotes cardioprotection via β-arrestin-biased agonism of β-adrenergic receptor (βAR).[10–13] MiR-532-5p (hereinafter referred to as miR-532) is one of the miRs that we found to be activated by Carv in the heart.[14] MiR-532 expression is dysregulated in a variety of conditions. For example, miR-532 is up-regulated in myoblasts from muscle

* Corresponding author. Tel: +1 706 721 9414; fax: +1 706 721 9799, E-mail: ilkim@augusta.edu

dystrophy patients,[15] serum from patients with deep vein thrombosis[16] and type 2 diabetes,[17] or human endothelial progenitor cells under hypoxic conditions,[18] while it is down-regulated in plasma from patients with chronic obstructive pulmonary disease[19] or fractures.[20] Although miR-532 has been implicated in the pathophysiology of certain cancers[21–23] and as a mediator of anti-viral host defence,[24] there is no evidence that miR-532 plays a functional role in the heart.

Prss23 is a serine protease and highly conserved in vertebrates. In aortic endothelial cells *in vitro* and in cardiac valve formation during zebrafish development, prss23 has been shown to induce Snail-mediated EndMT signalling,[25] a maladaptive process that was reported to inhibit cardiac neovascularization in pressure over-load and ischemia/reperfusion (I/R) mouse models.[26,27] Notably, *prss23* was significantly up-regulated in cancer stem cells[28] and has been associated with tumour progression in various types of cancers[29,30] as well as renal fibrosis.[31] Interestingly, we found that *prss23* was down-regulated in mouse hearts upon Carv stimulation.[32] However, whether this gene is functionally regulated by the Carv-responsive miR-532 and contributes to cardiac pathology is unknown.

Here, we show that knockdown of miR-532 alters the pathological responses of the heart in MI, and that miR-532 acts as a gatekeeper of cardiac vascularization by repressing a known EndMT initiator *prss23*. Therefore, miR-532 may represent a novel therapeutic target for combating ischemic heart injury.

2. Methods

2.1 Animal study

Eight to 12-week-old C57BL/6 wild-type (WT) mice were used for this study. Research with animals carried out for this study was performed according to approved protocols and animal welfare regulations of Augusta University's Institutional IACUC Committees. All animal procedures were performed in accordance with NIH guidelines. Mice were euthanized by thoracotomy under 1–4% inhalant isoflurane.

2.2 Histology and immunohistochemistry

The hearts were harvested and weighed before undergoing gross anatomical inspection. Morphometric analysis of the heart size was performed as previously published.[33] Histo-pathological analysis of the cardiac tissues, including fibrosis (Masson's trichrome staining), was performed using standard procedures as previously described.[34,35] For gross histological examination, sections were stained with haematoxylin and eosin (H and E). Myocardial sections were also stained for TUNEL to measure apoptosis using *In Situ* Cell Death Detection Kits (Roche) according to the manufacturer's instructions. The following anti-bodies were used to mark the cardiac endothelial cells (CECs) and cardiomyocytes (CMs), respectively: CD31, rabbit polyclonal (ab28364, Abcam), and Troponin I (TnI), rabbit polyclonal (sc-15368, Santa Cruz). To identify all active phases of cell cycle (G1, S, G2, and M) and mitosis, we used Ki67, rabbit polyclonal (ab15580, Abcam); and phospho-histone H3 (PH3), rabbit polyclonal (ab5176, Abcam) anti-bodies, respectively. We also used collagen type 1 α1 (COL1A1), mouse monoclonal (sc-293182, Santa Cruz), and α-smooth muscle actin (α-SMA), mouse monoclonal (ab7817, Abcam) anti-bodies to visualize myofibroblasts.

2.3 Statistical analysis

Data are expressed as mean ± SEM from at least three independent experiments with different biological samples per group. Statistical significance was determined using two-way ANOVA for two variables, one-way ANOVA with Bonferroni correction for multiple comparisons, or Student unpaired *t*-tests (GraphPad Prism version 5). A P value < 0.05 was considered statistically significant.

Other methods are provided in Supplementary material online.

3. Results

3.1 *In vivo* knockdown of miR-532 augments post-MI cardiac dysfunction and remodelling

To investigate the role of miR-532 in experimental MI, we intramyocardially injected locked nucleic acid (LNA)^{TM}-anti-miR-532 into WT mice immediately after left anterior descending (LAD) occlusion or sham surgery. First, we demonstrated efficacy of the anti-miR-532 by showing that the level of miR-532 was reduced (by ∼55%) after 7 days compared with anti-miR controls in both the sham and MI groups. We also observed down-regulation of miR-532 in the hearts of WT mice subjected to 1 week of MI (*Figure 1A*). We further showed that the hearts of anti-miR-532-injected mice at baseline were functionally normal (*Figure 1B–F* and see Supplementary material online, *Table S1–S3*). These findings suggest that miR-532 does not affect basal cardiac function in the absence of a pathological insult. Despite the normal phenotype at baseline, knockdown of miR-532 resulted in augmented cardiac dysfunction (as evidenced by significantly decreased EF, FS, and LVAWs as well as increased LVIDs and LVIDd), and increased ratios of HW/BW and LVW/BW at 3 days (*Figure 1B–F* and see Supplementary material online, *Table S2*), and 7 days (*Figure 1B–F* and see Supplementary material online, *Table S3*) after MI, when compared with controls. However, we did not observe a significant difference in mortality between anti-miR-532-injected mice and anti-miR controls following ligation of the LAD (data not shown).

We also found that anti-miR-532-injected hearts exhibited increased disorganized structure as well as loss of normal architecture and cellular integrity at 7 days post-MI as compared with anti-miR control hearts (*Figure 2A*), which is consistent with our biochemical data showing that knockdown of miR-532 led to increased mRNA levels of fetal genes and pro-inflammatory *TNF-α* compared with anti-miR controls (*Figure 2B, C* and see Supplementary material online, *Figure S1A–C*). To further assess the consequence of miR-532 knockdown following MI, we examined fibrosis by Masson's trichrome staining and by quantifying fibrotic gene expression. At 7 days post-MI, treatment with anti-miR-532 resulted in a much greater degree of fibrosis (*Figure 2D, E*), and increased mRNA levels of fibrotic *Col3a1* (*Figure 2F*), as compared with anti-miR controls.

We next demonstrated that anti-miR-532-injected hearts had higher numbers of TUNEL-positive cells in the heart sections at 7 days post-MI as compared with anti-miR controls (*Figure 3A, B*). This is consistent with our biochemical data showing increased mRNA levels of pro-apoptotic *Bax* following knockdown of miR-532 compared with controls (*Figure 3C*). Collectively, these results suggest that knockdown of miR-532 resulted in diverse pathological abnormalities during post-MI cardiac structural/functional remodelling.

3.2 *In vivo* knockdown of miR-532 reduces CEC proliferation and cardiac vascularization after MI

To further assess the effects of anti-miR-532, we examined cell proliferation post-MI using immunostaining for Ki-67 and phosphorylated

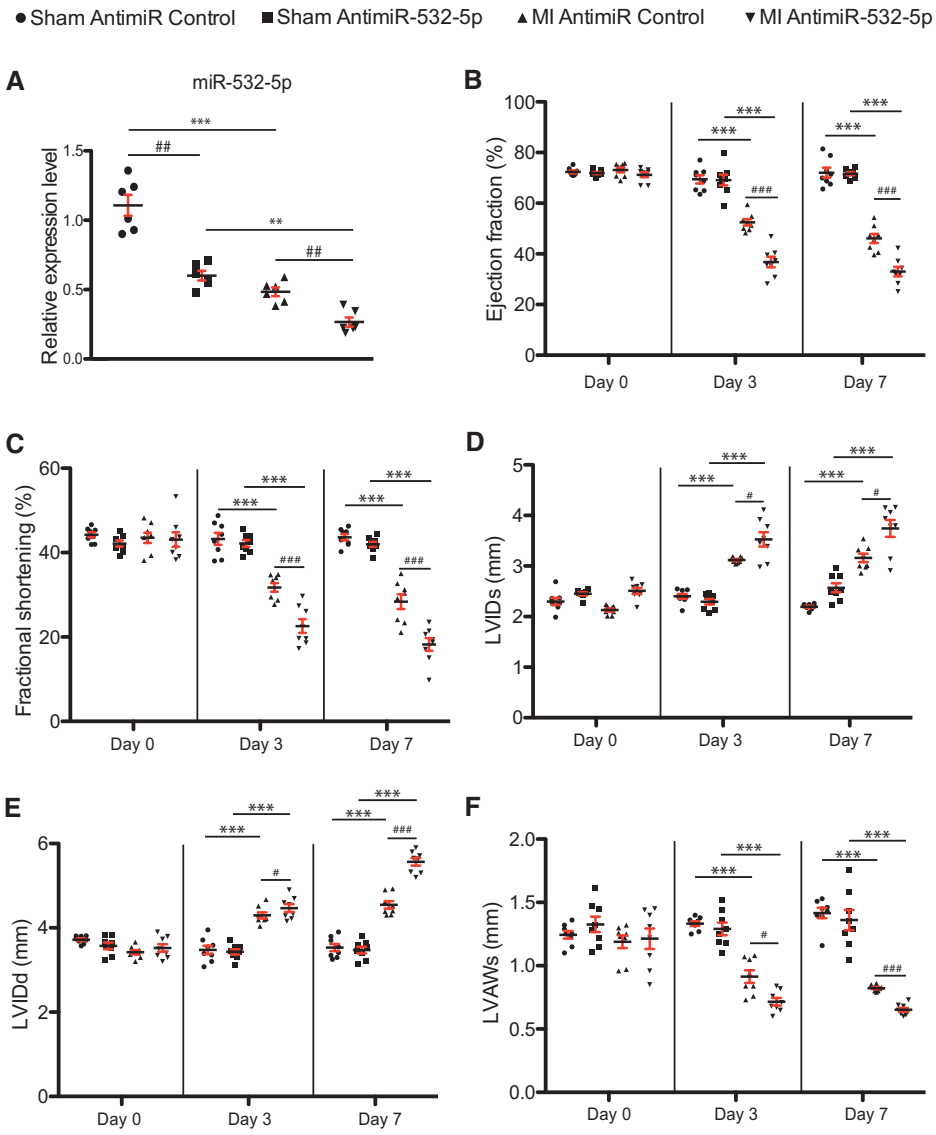

Figure 1 MiR-532 protects the mouse heart against MI. (*A*) QRT-PCR expression analysis of miR-532 in hearts from WT mice intramyocardially injected with 0.5 mg/kg of LNA^{TM} miR-532 inhibitor (anti-miR-532) or scrambled anti-miR control at 7 days post-MI. Data are shown as relative miR-532 expression normalized to U6 snRNA. (*B–F*) Transthoracic echocardiography was performed at 3 and 7 days post-MI by a blinded investigator on age/sex-matched mice. Quantification of left ventricular (LV) ejection fraction (*B*), fractional shortening (*C*), LV internal diameter, systole (LVIDs: *D*), LV internal diameter, diastole (LVIDd: *E*), and LV anterior wall thickness, systole (LVAWs: *F*) is shown. $N = 6–18$ per group; data represent mean ± SEM. $^{**}P < 0.01$, or $^{***}P < 0.001$ vs. Sham; $^{\#}P < 0.05$, $^{\#\#}P < 0.01$, or $^{\#\#\#}P < 0.001$ vs. anti-miR control.

histone H3 (PH3), which mark active phases of the cell cycle and mitosis, respectively. We detected reductions in both markers in hearts injected with anti-miR-532 compared with controls (see Supplementary material online, *Figure S2A, B* and *Figure 3D, E*). This is consistent with our biochemical data showing that anti-miR-532-injected hearts had decreased mRNA levels of S-phase marker *PCNA* and mitosis marker *Aurora B* compared with anti-miR controls (see Supplementary material online, *Figure S2C* and *Figure 3F*). To determine which cell types underwent less proliferation in anti-miR-532-injected hearts, we co-labelled heart sections to detect Ki-67 along with the CM marker TnI or the endothelial cell (EC) marker CD31. We found that knockdown of miR-532 resulted in lower numbers of Ki67-positive CECs, but not CMs, at 7 days after MI compared with controls (see Supplementary material online, *Figure S2D–F*). We next examined the expression of miR-532 in different myocardial cells. The expression of miR-532 was significantly higher in CECs than other myocardial cells and was selectively down-regulated in CECs isolated from ischemic myocardium at 1 week post-MI (*Figure 4A*). Both a previous cellular uptake study showing that injections of low doses of anti-miRs (such as 0.5 mg/kg used in our study) repressed miRs mainly in fractionated ECs in the heart[36] and this miR-532 expression data in myocardial cells (*Figure 4A*) correlated with our cell-type specific effect of miR-532 knockdown (see Supplementary material online, *Figure S2D–F*). Because we detected less CEC proliferation in anti-miR-532-injected hearts, we next tested the hypothesis that impaired CEC proliferation

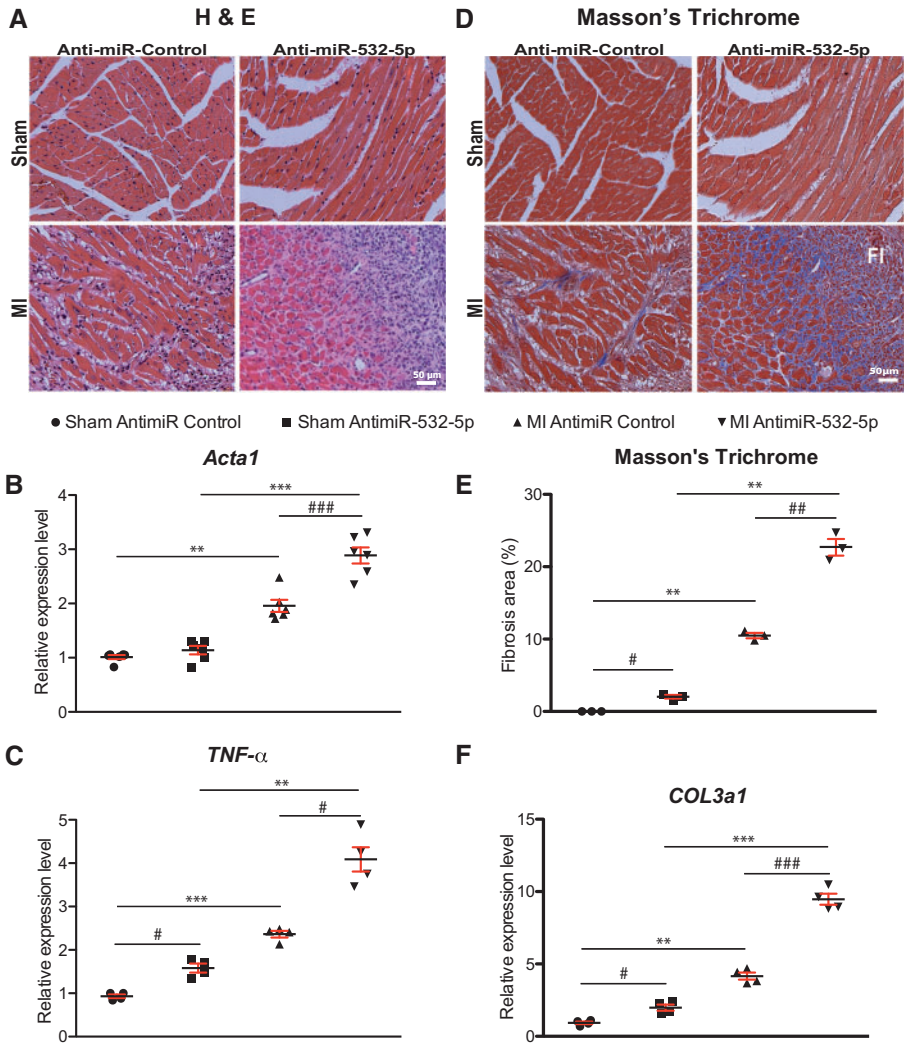

Figure 2 Knockdown of miR-532 induces abnormalities in cardiac structure, histology, and expression of genes involved in cardiac stress, pro-inflammation, and fibrosis. (*A*) Representative H & E staining of heart sections of peri-ischemic border area at 7 days post-MI demonstrates increased disorganized structure as well as loss of normal architecture and cellular integrity in anti-miR-532-injected hearts compared with anti-miR controls. (*B–C*) QRT-PCR analysis of gene expression (*Acta1*: cardiac stress and *TNF-α*: inflammation) in the post-infarcted hearts from anti-miR-532-injected mice compared with anti-miR controls at 7 days post-MI. (*D–E*) Representative Masson's trichrome staining (*D*) and quantification of fibrosis (FI; *E*) in heart sections of peri-ischemic border area at 7 days post-MI. The tissue sections shown in *A* (H & E) and *D* (Masson's trichrome) are anatomically contiguous for all four groups and adjacent sections are used for both staining protocols. (*F*) QRT-PCR analysis of fibrotic *Col3a1* expression in anti-miR-532-injected hearts relative to anti-miR controls at post-MI day 7. $N = 3–6$ per group; data are shown as relative gene expression normalized to HPRT1 or % of fibrosis area. $^{**}P < 0.01$ or $^{***}P < 0.001$ vs. sham; $^{\#}P < 0.05$, $^{\#\#}P < 0.01$, or $^{\#\#\#}P < 0.001$ vs. anti-miR control.

may contribute to increased fibrosis and cell death observed in anti-miR-532-injected hearts. Notably, both capillary density and the expression of EC markers were significantly reduced in anti-miR-532-injected hearts compared with anti-miR controls (*Figure 4B–E*), suggesting that miR-532 protects the myocardium in part through neovascularization after MI.

3.3 MiR-532 regulates a positive regulator of EndMT, prss23

In order to identify candidate miR-532 target genes that regulate cardiac pathology and impair CEC responses, we first used bioinformatic miRNA target prediction tools[37–39] and detected a substantial number of genes with putative binding sites for miR-532. Although functional miR binding sequences are often located in the 3′-untranslated region (3′-UTR) of target mRNA, it has been reported that the miR target can also occur with the 5′-UTR[40] or coding region.[41] By focusing our attention on predicted target genes that were also down-regulated in the mouse heart upon Carv stimulation in our previous study,[32] we identified *prss23* as a gene of interest among hundreds of possible targets. The rationale to focus on *prss23* is that Carv may inhibit the target by up-regulating miR-532. The sequence of miR-532 is conserved between mouse and human. Human *prss23* has two miR-532 binding sites (one strong site with 7 bp seed length and one weak site with 6 bp seed length based on miRanda) and one strong binding site with 7 bp seed length (based on

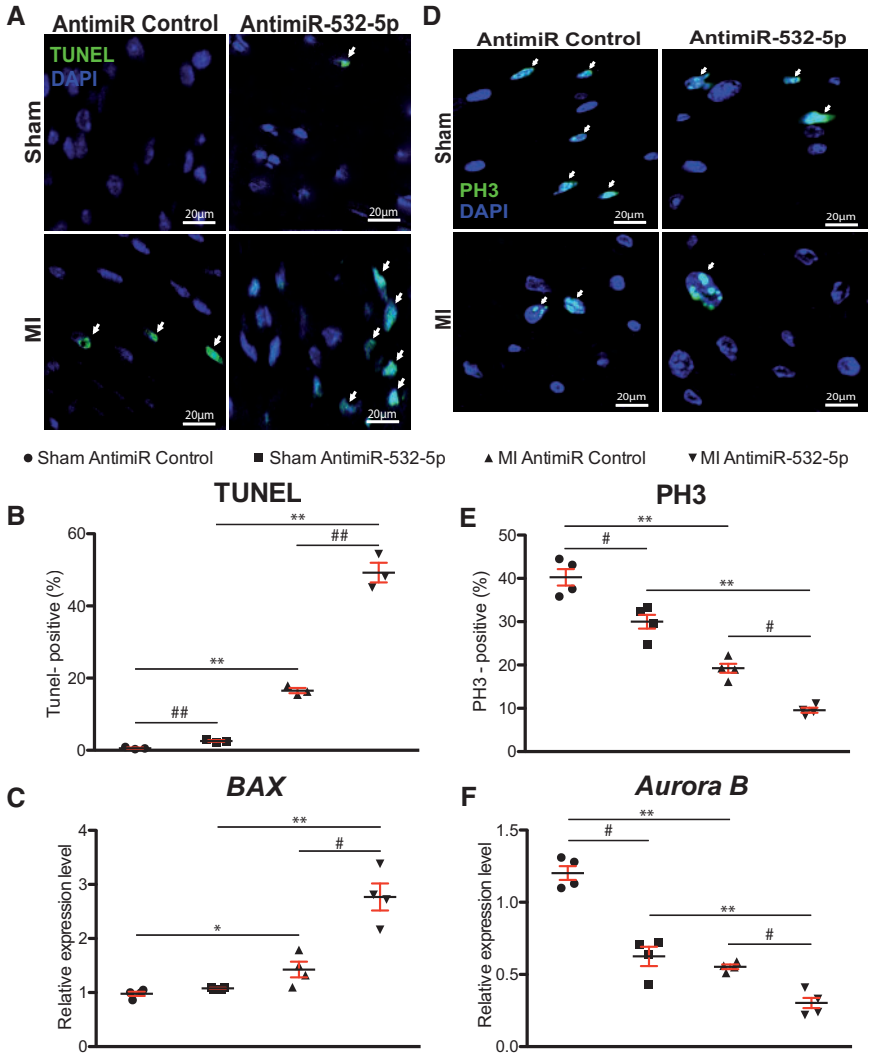

Figure 3 MiR-532 knockdown increases cardiac apoptosis but decreases cardiac cell proliferation post-MI. (*A*, *B*), Representative TUNEL staining (*A*) and quantification (*B*) of transverse heart sections of peri-ischemic border area at 7 days post-MI show increased apoptosis in anti-miR-532-injected hearts compared with anti-miR controls. (*C*) QRT-PCR expression analysis of apoptotic *Bax* in anti-miR-532-injected hearts relative to anti-miR controls at 7 days post-MI. (*D*, *E*) Representative phospho-histone 3 (PH3: proliferation marker at M phase of cell cycle) staining (*D*) and quantification (*E*) of transverse heart sections of peri-ischemic border area at 7 days post-MI show decreased proliferation in anti-miR-532-injected hearts compared with anti-miR controls. (*F*) QRT-PCR expression analysis of a mitotic marker *Aurora B* in anti-miR-532-injected hearts relative to anti-miR controls at 7 days post-MI. $N = 3$–4 per group; data are shown as relative gene expression normalized to HPRT1 or % of positive cells. $^{*}P < 0.05$ or $^{**}P < 0.01$ vs. sham; $^{\#}P < 0.05$ or $^{\#\#}P < 0.01$ vs. anti-miR control.

TargetScan) in its 3′-UTR. Although mouse *prss23* 3′UTR does not have the miR-532 binding site, mouse *prss23* possesses a strong miR-532 binding site with 7 bp seed length in its 5′-UTR (based on miRWalk and RNAhybrid), suggesting evolutionary conservation of miR-532's regulation of prss23 and their roles between mouse and human despite different target locations. This idea is supported by a previous finding demonstrating that the function of prss23 in valvulogenesis is evolutionarily conserved.[25]

Prss23 is a serine protease that was reported to regulate EndMT in aortic ECs *in vitro* and cardiac valve formation during zebrafish development *in vivo* via inducing Snail1-mediated EndMT signalling.[25] To validate *prss23* as a novel functional target of miR-532 in CECs and hearts, we first measured the mRNA and protein levels of prss23, as well as downstream Snail1 protein levels, in anti-miR-532-injected hearts. We showed that anti-miR-532-injected mouse hearts exhibited significant up-regulation of mRNA and protein levels of prss23 both at baseline and 7 days post-MI compared with controls (*Figure 5A–C*), suggesting that miR-532 promotes the degradation of *prss23* mRNA. The protein level of Snail1, which is activated by prss23 in EndMT,[25] was also increased in anti-miR-532 MI group compared with anti-miR controls (*Figure 5B, C*). We also found that *runx3* was up-regulated in anti-miR-532-injected hearts both at baseline and 7 days post-MI compared with controls (see Supplementary material online, *Figure S3A*). Interestingly, runx3 has been identified as a direct target of miR-532 in gastric cancer,[23] and it is also known to promote EndMT by inducing Slug.[42] Importantly, we demonstrated that miR-532 expression is down-regulated in the hearts of WT mice subjected to 3, 5,

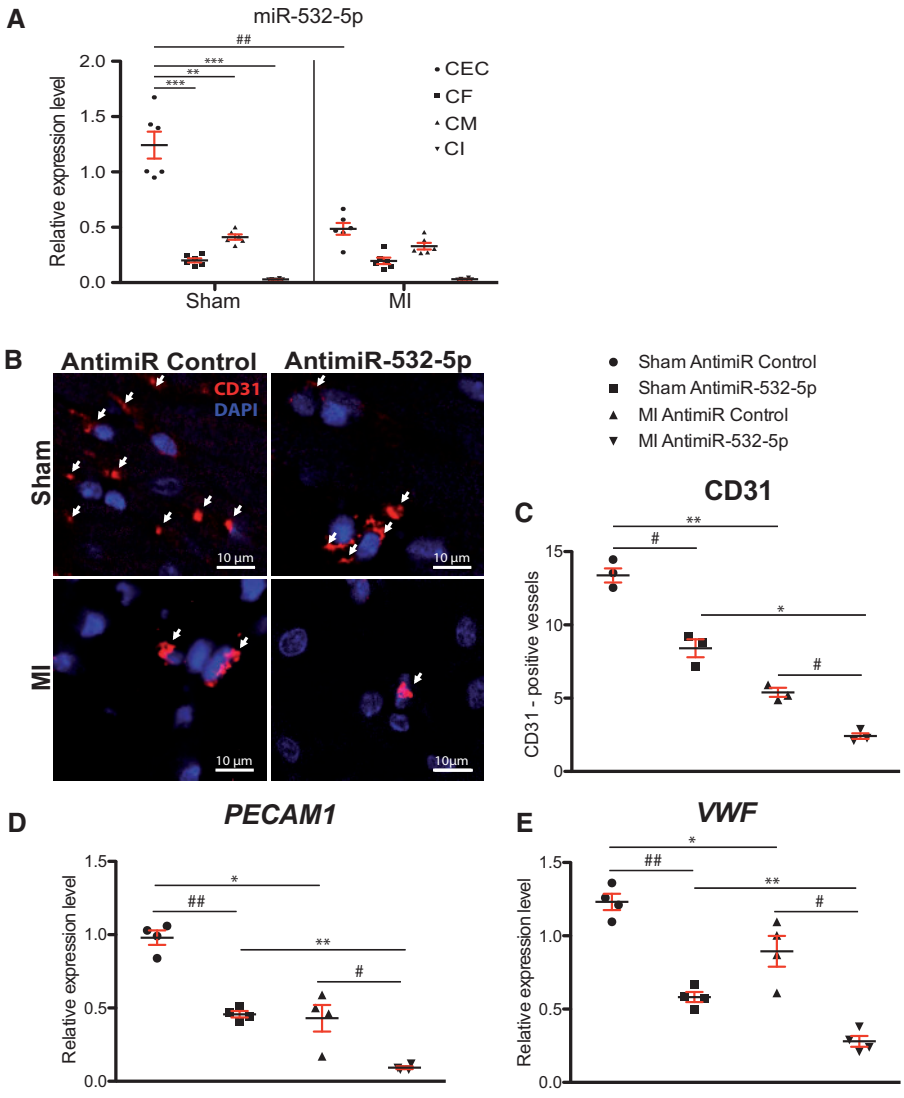

Figure 4 MiR-532 is highly expressed in cardiac endothelial cells and miR-532 knockdown reduces cardiac vascularization after MI. (*A*) The expression of miR-532 in cardiomyocytes (CMs), cardiac fibroblasts (CFs), endothelial cells (CECs), and inflammatory cells (CIc) from adult mouse heart was detected by real time RT-PCR. $N = 6$. $^{**}P < 0.01$ or $^{***}P < 0.001$ vs. CECs. $^{\#\#}P < 0.001$ vs. sham. (*B*, *C*) Representative CD31 staining (*B*) and quantification (*C*) of transverse heart sections of peri-infarct zone at 7 days post-MI show decreased vessels in anti-miR-532-injected hearts compared with anti-miR controls. (*D*, *E*) QRT-PCR expression analysis of endothelial *PECAM1* (*D*) and *VWF* (*E*) in anti-miR-532-injected hearts relative to anti-miR controls at 7 days post-MI. $N = 3$–4 per group; data are shown as relative gene expression normalized to HPRT1 or #s of positive vessels. $^{*}P < 0.05$ or $^{**}P < 0.01$ vs. sham; $^{\#}P < 0.05$ or $^{\#\#}P < 0.01$ vs. anti-miR control.

and 7 days of MI compared with controls (see Supplementary material online, *Figure S3B*), while cardiac expression of *prss23* was concomitantly up-regulated (see Supplementary material online, *Figure S3C*). Interestingly, the expression of *prss23* in CECs was significantly lower than other myocardial cells and selectively up-regulated in CECs isolated from ischemic myocardium at 7 days post-MI (*Figure 5D*), which is inversely associated with the expression of miR-532 (*Figure 4A*).

To test whether prss23 is a direct target of miR-532 repression, we co-transfected CECs with constitutively active luciferase reporter constructs containing 3′UTR of *prss23* (*Figure 5E*) and miR-532 mimic. We observed repression of luciferase activity by miR-532 for the *prss23*-3′UTR reporter. Mutation of seed binding sites for miR-532 made the reporter insensitive to miR-532 over-expression (*Figure 5F*), indicating the specific dependence of target 3′-UTR on miR-532. Together with our previous studies demonstrating that Carv decreased the expression of *prss23* concordant with up-regulation of miR-532,[14,32] our current results showing an inverse relationship during MI strongly suggest that prss23 is an important direct target of miR-532 in the heart.

3.4 MiR-532 functions as a protective miR by repressing a positive EndMT regulator, prss23 in CECs

Because our data suggest that prss23, a key promoter of EndMT is a novel direct target of miR-532, we hypothesized that miR-532 may inhibit EndMT, subsequently decreasing cardiac fibroblastic content and

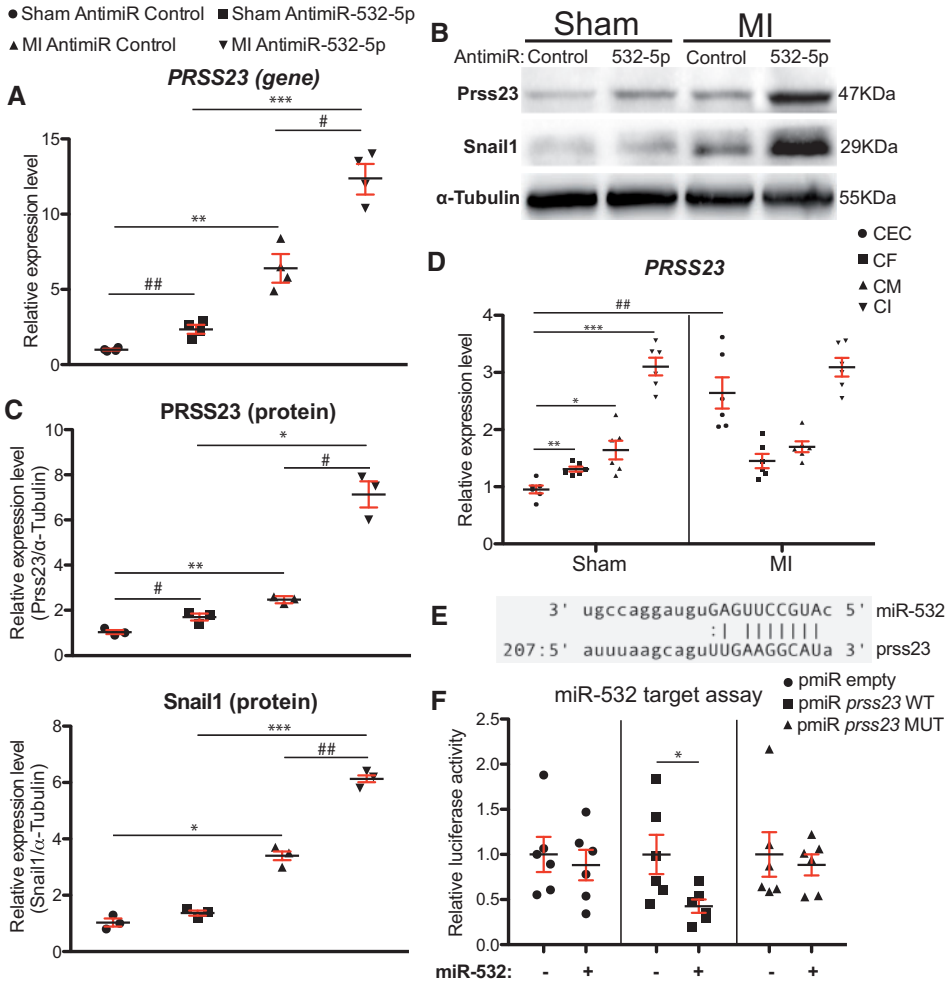

Figure 5 MiR-532 represses a detrimental EndMT marker *prss23* and *prss23* is a novel direct target of miR-532. (*A*) *Prss23* mRNA levels were measured in lysates of left ventricular tissues from anti-miR-532-injected mice compared with anti-miR controls at baseline and 7 days post-MI. (*B*, *C*) Prss23 and downstream Snail1 protein levels were measured lysates of left ventricular tissues from anti-miR-532-injected mice compared with anti-miR controls at baseline and 7 days post-MI. $N = 3–4$. $^{*}P < 0.05$, $^{**}P < 0.01$, or $^{***}P < 0.001$ vs. sham; $^{\#}P < 0.05$ or $^{\#\#}P < 0.05$ vs. anti-miR control. (*D*) The expression of *prss23* in cardiomyocytes (CMs), cardiac fibroblasts (CFs), endothelial cells (CECs), and inflammatory cells (CIc) from adult mouse heart was detected by real time RT-PCR. $^{*}P < 0.05$, $^{**}P < 0.01$, or $^{***}P < 0.001$ vs. CECs. $^{\#\#}P < 0.01$ vs. sham. (*E*) Human prss23 has a strong miR-532 binding site at its 3′-UTR. MiR-532 seed pairing in the target region is shown as vertical lines. (*F*) Ability of miR-532 to directly repress the activity of luciferase reporter constructs that contain either WT 3′-UTR or mutated (MUT) 3′-UTR for prss23. Transfection with or without miR-532 mimic is indicated. Firefly luciferase activity was normalized to Renilla luciferase activity and compared with empty vector measurements. $N = 6$. $^{*}P < 0.05$ vs. miR mimic control.

promoting cardiac vascularization. To examine the potential role of miR-532 in EndMT, we first performed double staining for COL1A1 or α-SMA and CD31 in heart sections of anti-miR-532-injected mice and anti-miR controls. We observed that anti-miR-532-injected mouse hearts exhibited an increase of both COL1A1/CD31 and α-SMA/CD31 double-positive cells both at baseline and 7 days post-MI compared with controls (see Supplementary material online, *Figure S4*). Combined with *Figures 2D–F* and *4B–E* showing that anti-miR-532-injected hearts had increased cardiac fibroblastic content and deceased cardiac vascularization, our data suggest that miR-532 inhibits EC conversion into fibroblast-like cells (i.e. EndMT) in the heart.

It is known that prss23 modulates Snail1 transcription to promote TGF-β2-mediated EndMT initiation in human aortic ECs,[25] and that only ECs and macrophages uptake acetylated-LDL (ac-LDL).[43] To determine the importance of miR-532 for TGF-β2-mediated EndMT in CECs, we exposed MCECs to TGF-β2 for 7 days and then labelled them with Dil-Ac-LDL. Knockdown of miR-532 in MCECs decreased Dil-Ac-LDL uptake (see Supplementary material online, *Figure S5A, B*), indicating a loss of endothelial functionality. Moreover, knockdown of miR-532 resulted in decreased expression of *VWF* and CD31 in the absence and presence of TGF-β2 compared with anti-miR controls (see Supplementary material online, *Figures S5C* and *S6B, C*), while expression of *Col3a1*, *Snail1*, and α-SMA was up-regulated in the presence of TGF-β2 (see Supplementary material online, *Figures S5D* and *S6A, B,* and *D*). These results suggest that knockdown of miR-532 in CECs promotes transition to a fibroblast-like phenotype via EndMT.

To begin to address the therapeutic potential of miR-532, we next investigated whether miR-532 over-expression is beneficial in preventing

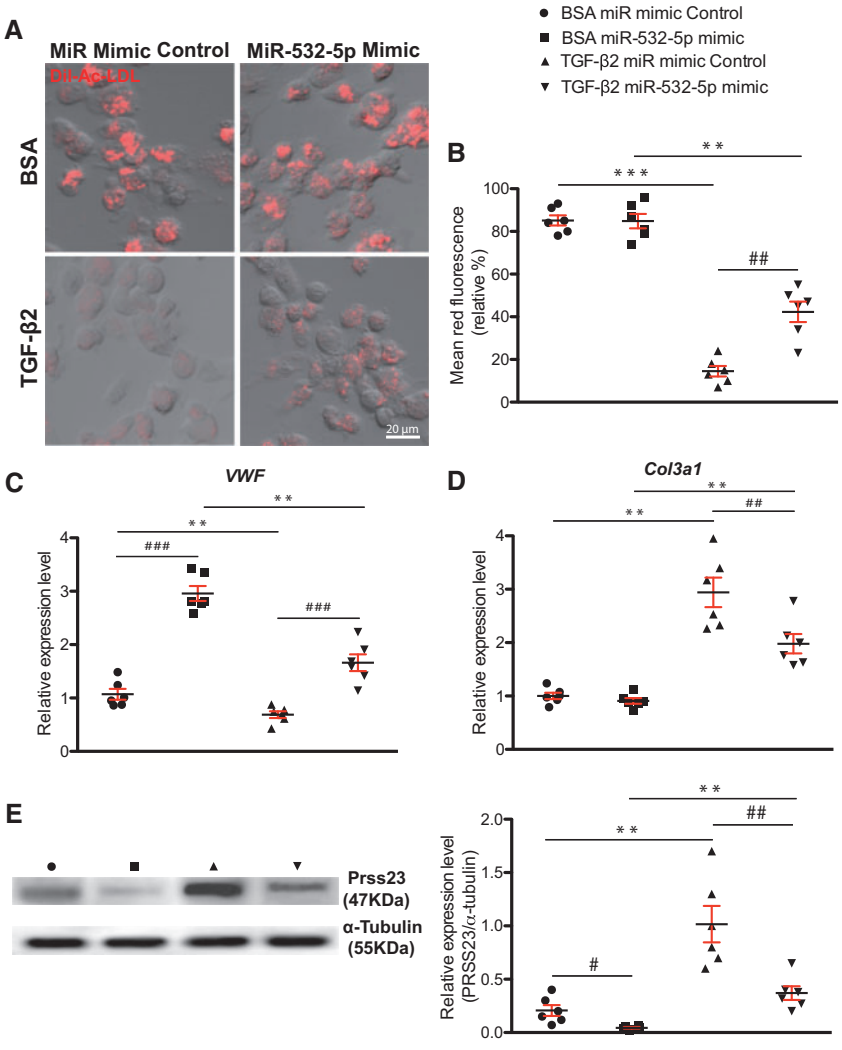

Figure 6 MiR-532 over-expression inhibits EndMT in CECs. (*A*, *B*) Mouse cardiac endothelial cells (MCECs) were treated with TGF-β2 or BSA (vehicle) for 7 days in the presence of either miR-532-5p mimic or miR mimic control. MCECs transfected with miR-532-5p mimic showed significant increase in receptor-mediated endocytosis of Dil-Ac-LDL after TGF-β2 treatment vs. miR mimic control, demonstrating gain of endothelial phenotype and loss of mesenchymal phenotype. (*C*, *D*) QRT-PCR expression analysis of endothelial *VWF* (*C*) or fibrotic *Col3a1* (*D*) in miR-532 mimic-transfected MCECs relative to miR mimic controls. (*E*) Immunoblotting analysis of prss23 in MCECs subjected as aforementioned in *A*–*D*. $N = 6$. $^{**}P < 0.01$ or $^{***}P < 0.001$ vs. BSA; $^{\#}P < 0.05$, $^{\#\#}P < 0.01$, or $^{\#\#\#}P < 0.001$ vs. miR mimic control.

EndMT and induction of prss23 in CECs. Over-expression of miR-532 in MCECs increased Dil-Ac-LDL uptake in the presence of TGF-β2 (*Figure 6A, B*), indicating a gain of endothelial functionality. Moreover, over-expression of miR-532 resulted in increased expression of *VWF* in the absence or presence of TGF-β2 compared with miR mimic controls, while expression of *Col3a1* and prss23 was down-regulated in the presence of TGF-β2 (*Figure 6C–E*). We next determined if the target of miR-532, prss23 regulates EndMT in CECs. Loss-of-function approaches demonstrated that compared with controls, knockdown of prss23 increased Dil-Ac-LDL uptake (see Supplementary material online, *Figure S7A* and *Figure 7A, B*), expression of *VWF* (see Supplementary material online, *Figure S7C*) and CD31 (*Figure 7C, D*) in response to TGF-β2, and decreased expression of *Snail1*, *Col3a1*, and α-SMA in the presence of TGF-β2 (see Supplementary material online, *Figure S7D, E*, and *Figure 7C* and *E*). Our results suggest that prss23 is sufficient to promote TGF-β2-mediated EndMT in CECs. Finally, to establish a functional linkage between miR-532, prss23 expression, and EndMT, we applied a siRNA/anti-miR-based rescue strategy to validate the functional relevance of the novel miR-532 target. Consistent with our earlier observations (see Supplementary material online, *Figure S5A–D*), anti-miR-532 treatment promoted EndMT, which was blocked by siRNA against prss23 (*Figure 7A–E* and see Supplementary material online, *Figure S7A–E*). Taken together, our CEC data support the *in vivo* evidence that miR-532 exerts cardioprotective effects in part through functional repression of a positive regulator of EndMT, prss23.

4. Discussion

Here, we identify miR-532 as a stress-responsive protector against EndMT both *in vivo* and *in vitro*. Knockdown of miR-532 in the heart

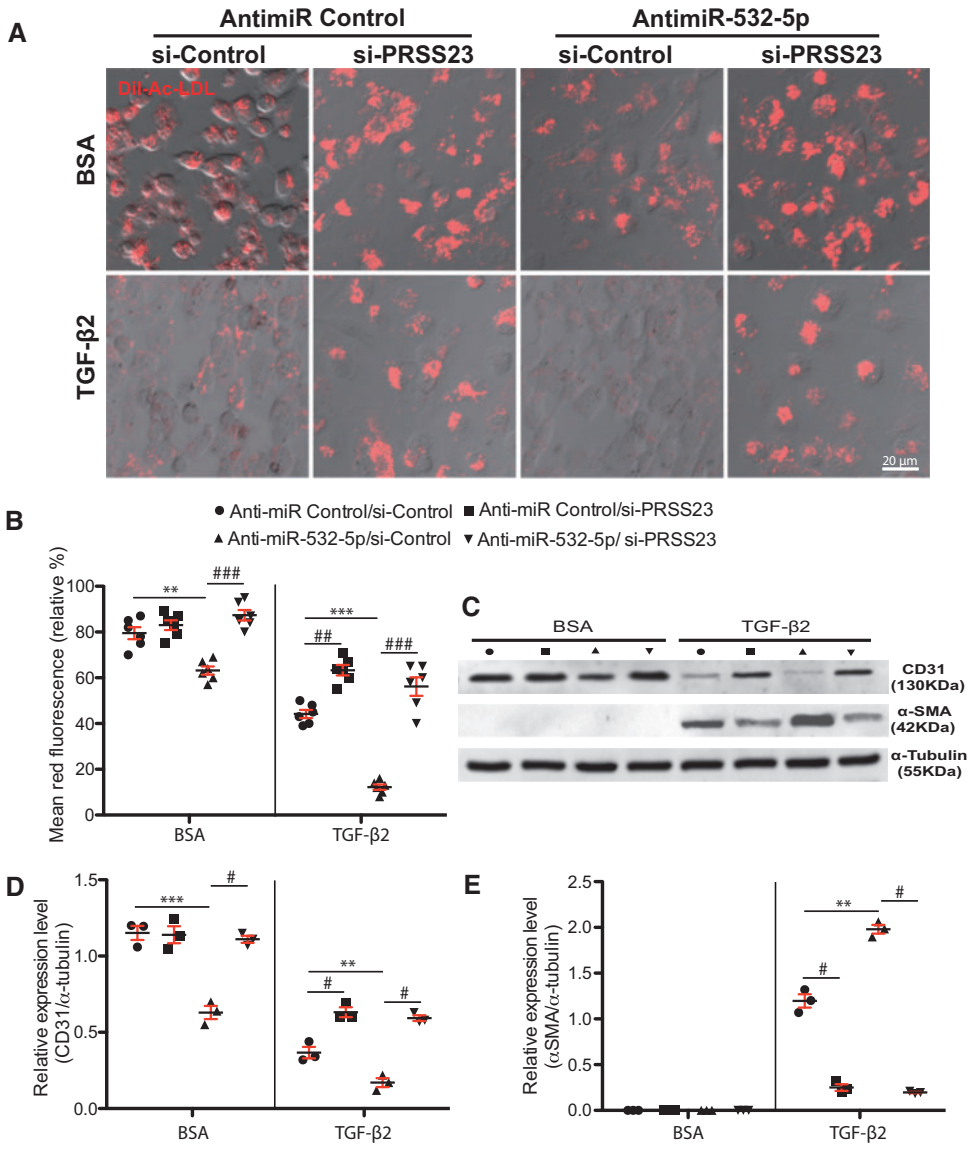

Figure 7 Prss23 is necessary for miR-532-dependent regulation of EndMT. (*A*, *B*) MCECs transfected with control scramble siRNA (si-control), prss23 siRNA (si-Prss23), or anti-miR-532/si-Prss23 were treated with TGF-β2 or BSA (vehicle) for 7 days. Dil-Ac-LDL labelling was then performed. Knockdown of prss23 increases receptor-mediated endocytosis of Dil-Ac-LDL and protects MCECs from the TGF-β2-mediated EndMT effects of anti-miR-532. (*C*–*E*) Immunoblotting analysis of endothelial CD31 (*C*, *D*) or mesenchymal α-SMA (*C* and *E*) in MCECs subjected as aforementioned in *A*, *B*. $N = 3$–6. $^{**}P < 0.01$ or $^{***}P < 0.001$ vs. anti-miR control/si-control; $^{\#}P < 0.05$, $^{\#\#}P < 0.01$, or $^{\#\#\#}P < 0.01$ vs. anti-miR control/si-control or anti-miR-532/si-control.

augments injury in the setting of MI, as evidenced by increased cardiac cell death and fibrosis, decreased CEC proliferation and cardiac vascularization, and impairment of ventricular function. Mechanistically, we determined that miR-532 targets an EndMT initiator prss23 to, at least in part, elicit its protective effects. *In vitro*, CECs deficient in miR-532 exhibit increased sensitivity to TGF-β2-mediated EndMT, while CECs over-expressing miR-532 display decreased EndMT.

EndMT is a key mechanism by which cardiac fibroblasts increase production of extracellular matrix proteins and is characterized by loss of cell junctions and CD31 expression as well as up-regulated expression of mesenchymal markers such as α-SMA.[43] EndMT has been shown to significantly contribute to cardiac fibrosis and heart failure in pressure-induced cardiac damage,[26,44] while the opposite process of mesenchymal-to-endothelial transition (MEndT) was shown to contribute to cardiac neovascularization in cardiac I/R injury.[27] Although miR-200b was reported to mediate EndMT in diabetic cardiomyopathy,[45] a pathophysiologic role of other miRs in regulating EndMT in the heart has not been previously demonstrated. In the current study, we show that miR-532 reduces expression of *Snail1*, *Col3a1*, and α-SMA in the heart and CEC, while increasing expression of *Pecam1*, *VWF*, and CD31, confirming a role of this miR in EndMT. Our COL1A1 or α-SMA/CD31 double staining data also support that miR-532 inhibits CEC conversion into myofibroblasts in the heart. We further show that miR-532 confers cardioprotective effects against MI in part by directly repressing a key EndMT initiator, prss23. Prss23 is essential for the initiation of EndMT via Snail1 during cardiac valvulogenesis, and this prss23-mediated

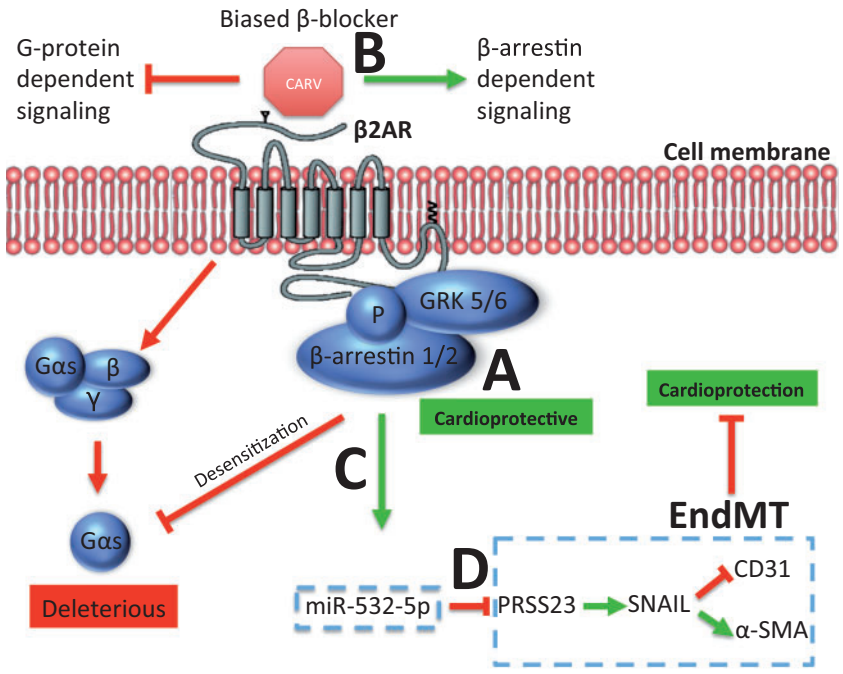

Figure 8 A β_2-adrenergic receptor (β_2AR)/β-arrestin-responsive miR, miR-532, is a novel mediator of cardioprotection by repressing an EndMT initiator prss23. β-Arrestin-mediated β_2AR signalling confers cardioprotective effects[13,46] (*A*) and the β-blocker carvedilol (Carv) is a β-arrestin-biased ligand for β_2AR[12] (*B*). Our previous microarray data showed that Carv induces the expression of miR-532[14] (*C*). Here, our results suggest that β-arrestin-biased agonism of β_2AR-mediated miR-532 activation is a novel cardioprotective mechanism, and that miR-532 confers cardioprotection by directly repressing an EndMT initiator *prss23* in CECs (*D*).

mechanism is evolutionally conserved.[25] Whether miR-532 regulates EndMT via additional regulatory mechanisms in the context of MI is unknown and beyond the scope of the current investigation.

We previously showed that miR-532 is activated by Carv,[14] which is a β-arrestin-biased ligand for β_2AR.[12] Our data also suggest that miR-532 is post-transcriptionally activated by β-arrestin-mediated β_2AR signalling pathways (data not shown), which have recently been identified to promote cardioprotective effects[13,46] (*Figure 8A–C*). Together with the results presented here (*Figure 8D*), we postulate that β-arrestin-biased β_2AR regulatory mechanism of miR biogenesis may result in beneficial adaptive remodelling following MI. This hypothesis is further supported by the observation that other Carv/β-arrestin1-regulatable miRs that we identified[14] are cardioprotective *in vivo* after I/R injury or MI.[33,47–49] Interestingly, two other studies linking Carv treatment to up-regulation of cardioprotective miRs have been also reported in MI.[50,51] Basal expression of the cardioprotective miR-133[52,53] in myocardial tissue was significantly up-regulated by Carv treatment, and up-regulation of miR-133 mediated the anti-apoptotic action of Carv in isolated CMs.[50] The up-regulation of miR-29b, another cardioprotective miR,[54] was also shown to contribute to the effects of Carv to attenuate post-MI fibrosis.[51] Collectively, these studies support the concept that the cardioprotective actions of Carv are associated with increased levels of cardioprotective miRs. Future studies are needed to fully elucidate the possible over-lapping/compensatory effects of known Carv-responsive miRs and their underlying mechanisms of action.

Prss23 is expressed in multiple organs in developing fetuses and adults, and is involved in tissue remodelling in the mouse ovary[55] and estrogen-dependent proliferation in breast cancer.[30] Interestingly, its expression is relatively high in the human fetal heart and up-regulated during mouse cardiac development. Prss23 has been reported to mediate EndMT signalling in aortic ECs during cardiac valvulogenesis.[25] In this study, we demonstrate for the first time that prss23 is a functional and direct CEC target of miR-532. Prss23 expression was reported to be up-regulated in cancer stem cells[28] and has been associated with tumour progression in various types of cancers[29,30] as well as renal fibrosis.[31] Our findings of up-regulation of *prss23* during MI (see Supplementary material online, *Figure S3C*) further support that inhibition of this gene could be therapeutically beneficial for cardiac disease although the role of prss23 *in vivo* needs to be determined. Given our data that this detrimental gene is a functional and direct CEC target of miR-532, and that there is an inverse correlation between miR-532 and prss23 during MI, up-regulating miR-532 (via Carv or miR-532 over-expression) could be a particularly attractive adjunctive approach to limiting peri-infarct damage and promoting recovery post-MI. However, these studies need to be done before considering this miR as a therapeutic option.

In conclusion, our results using loss-of-function approaches demonstrate for the first time that miR-532 protects the heart against MI in part by blunting EndMT in response to injury through its direct repression of prss23 (*Figure 8D*). We identified miR-532 as a critical regulator of CEC proliferation and cardiac vascularity after MI. We found miR-532 to be highly expressed in fractionated CECs and to be down-regulated after ischemic injury. However, miR-532 is also expressed in other myocardial cells. This finding, coupled with the excessive post-MI cardiac remodelling resulting from knockdown of miR-532, suggest a possible EC-

independent role for miR-532 in cardioprotection. Although additional *in vivo* functional and mechanistic studies concentrating on miR-532 in other cardiac cell types are needed to identify other potential mechanisms of miR-532-mediated cardioprotection, our data nevertheless suggest that boosting miR-532 levels in part to attenuate EndMT may beneficially regulate EC function to improve vascularity and cardiac performance after ischemic injury.

Supplementary material

Supplementary material is available at *Cardiovascular Research* online.

Conflict of interest: none declared.

Funding

This work was supported by American Heart Association Predoctoral Fellowship 16PRE30210016 to J.-p.T., National Institutes of Health R01 HL086555 to Y.T., National Institutes of Health R01 HL124248 to H.S., National Institutes of Health R01 HL134354 and AR070029 to Y.T. and N.L.W., National Institutes of Health R01 HL112640 and HL126949 to N.L.W., and American Physiological Society Shih-Chun Wang Young Investigator Award, American Heart Association Grant-in-Aid 12GRNT12100048 and Scientist Development Grant 14SDG18970040, and National Institutes of Health R01 HL124251 to I.-m.K.

References

1. Takemura G, Fujiwara H. Role of apoptosis in remodeling after myocardial infarction. *Pharmacol Ther* 2004;**104**:1–16.
2. Krijnen PA, Nijmeijer R, Meijer CJ, Visser CA, Hack CE, Niessen HW. Apoptosis in myocardial ischaemia and infarction. *J Clin Pathol* 2002;**55**:801–811.
3. Aisagbonhi O, Rai M, Ryzhov S, Atria N, Feoktistov I, Hatzopoulos AK. Experimental myocardial infarction triggers canonical Wnt signaling and endothelial-to-mesenchymal transition. *Dis Model Mech* 2011;**4**:469–483.
4. Saraste A, Koskenvuo JW, Saraste M, Parkka J, Toikka J, Naum A, Ukkonen H, Knuuti J, Airaksinen J, Hartiala J. Coronary artery flow velocity profile measured by transthoracic Doppler echocardiography predicts myocardial viability after acute myocardial infarction. *Heart* 2007;**93**:456–457.
5. Kaul S, Jayaweera AR. Myocardial capillaries and coronary flow reserve. *J Am Coll Cardiol* 2008;**52**:1399–1401.
6. Arunachalam G, Upadhyay R, Ding H, Triggle CR. MicroRNA signature and cardiovascular dysfunction. *J Cardiovasc Pharmacol* 2015;**65**:419–429.
7. Maegdefessel L. The emerging role of microRNAs in cardiovascular disease. *J Intern Med* 2014;**276**:633–644.
8. van Rooij E, Marshall WS, Olson EN. Toward microRNA-based therapeutics for heart disease: the sense in antisense. *Circ Res* 2008;**103**:919–928.
9. Catalucci D, Gallo P, Condorelli G. MicroRNAs in cardiovascular biology and heart disease. *Circ Cardiovasc Genet* 2009;**2**:402–408.
10. Kim IM, Tilley DG, Chen J, Salazar NC, Whalen EJ, Violin JD, Rockman HA. Beta-blockers alprenolol and carvedilol stimulate beta-arrestin-mediated EGFR transactivation. *Proc Natl Acad Sci U S A* 2008;**105**:14555–14560.
11. Noma T, Lemaire A, Naga Prasad SV, Barki-Harrington L, Tilley DG, Chen J, Le Corvoisier P, Violin JD, Wei H, Lefkowitz RJ, Rockman HA. Beta-arrestin-mediated beta1-adrenergic receptor transactivation of the EGFR confers cardioprotection. *J Clin Invest* 2007;**117**:2445–2458.
12. Wisler JW, DeWire SM, Whalen EJ, Violin JD, Drake MT, Ahn S, Shenoy SK, Lefkowitz RJ. A unique mechanism of beta-blocker action: carvedilol stimulates beta-arrestin signaling. *Proc Natl Acad Sci U S A* 2007;**104**:16657–16662.
13. Carr R 3rd, Schilling J, Song J, Carter RL, Du Y, Yoo SM, Traynham CJ, Koch WJ, Cheung JY, Tilley DG, Benovic JL. Beta-arrestin-biased signaling through the beta2-adrenergic receptor promotes cardiomyocyte contraction. *Proc Natl Acad Sci U S A* 2016;**113**:E4107–E4116.
14. Kim IM, Wang Y, Park KM, Tang Y, Teoh JP, Vinson J, Traynham CJ, Pironti G, Mao L, Su H, Johnson JA, Koch WJ, Rockman HA. Beta-arrestin1-biased beta1-adrenergic receptor signaling regulates microRNA processing. *Circ Res* 2014;**114**:833–844.
15. Dmitriev P, Stankevicins L, Ansseau E, Petrov A, Barat A, Dessen P, Robert T, Turki A, Lazar V, Labourer E, Belayew A, Carnac G, Laoudj-Chenivesse D, Lipinski M, Vassetzky YS. Defective regulation of microRNA target genes in myoblasts from facioscapulohumeral dystrophy patients. *J Biol Chem* 2013;**288**:34989–35002.
16. Qin J, Liang H, Shi D, Dai J, Xu Z, Chen D, Chen X, Jiang Q. A panel of microRNAs as a new biomarkers for the detection of deep vein thrombosis. *J Thromb Thrombolysis* 2015;**39**:215–221.
17. Ortega FJ, Mercader JM, Moreno-Navarrete JM, Rovira O, Guerra E, Esteve E, Xifra G, Martinez C, Ricart W, Rieusset J, Rome S, Karczewska-Kupczewska M, Straczkowski M, Fernandez-Real JM. Profiling of circulating microRNAs reveals common microRNAs linked to type 2 diabetes that change with insulin sensitization. *Diabetes Care* 2014;**37**:1375–1383.
18. Mo J, Zhang D, Yang R. MicroRNA-195 regulates proliferation, migration, angiogenesis and autophagy of endothelial progenitor cells by targeting GABARAPL1. *Biosci Rep* 2016;**36**:e00396.
19. Soeda S, Ohyashiki JH, Ohtsuki K, Umezu T, Setoguchi Y, Ohyashiki K. Clinical relevance of plasma miR-106b levels in patients with chronic obstructive pulmonary disease. *Int J Mol Med* 2013;**31**:533–539.
20. Kocijan R, Muschitz C, Geiger E, Skalicky S, Baierl A, Dormann R, Plachel F, Feichtinger X, Heimel P, Fahrleitner-Pammer A, Grillari J, Redl H, Resch H, Hackl M. Circulating microRNA signatures in patients with idiopathic and postmenopausal osteoporosis and fragility fractures. *J Clin Endocrinol Metab* 2016:jc20162365.
21. Wang F, Chang JT, Kao CJ, Huang RS. High expression of miR-532-5p, a tumor suppressor, leads to better prognosis in ovarian cancer both in vivo and in vitro. *Mol Cancer Ther* 2016;**15**:1123–1131.
22. Song X, Wang Z, Jin Y, Wang Y, Duan W. Loss of miR-532-5p in vitro promotes cell proliferation and metastasis by influencing CXCL2 expression in HCC. *Am J Transl Res* 2015;**7**:2254–2261.
23. Xu X, Zhang Y, Liu Z, Zhang X, Jia J. miRNA-532-5p functions as an oncogenic microRNA in human gastric cancer by directly targeting RUNX3. *J Cell Mol Med* 2016;**20**:95–103.
24. Slonchak A, Shannon RP, Pali G, Khromykh AA. Human microRNA miR-532-5p exhibits antiviral activity against west Nile virus via suppression of host genes SESTD1 and TAB3 required for virus replication. *J Virol* 2016;**90**:2388–2402.
25. Chen IH, Wang HH, Hsieh YS, Huang WC, Yeh HI, Chuang YJ. PRSS23 is essential for the Snail-dependent endothelial-to-mesenchymal transition during valvulogenesis in zebrafish. *Cardiovasc Res* 2013;**97**:443–453.
26. Zeisberg EM, Tarnavski O, Zeisberg M, Dorfman AL, McMullen JR, Gustafsson E, Chandraker A, Yuan X, Pu WT, Roberts AB, Neilson EG, Sayegh MH, Izumo S, Kalluri R. Endothelial-to-mesenchymal transition contributes to cardiac fibrosis. *Nat Med* 2007;**13**:952–961.
27. Ubil E, Duan J, Pillai IC, Rosa-Garrido M, Wu Y, Bargiacchi F, Lu Y, Stanbouly S, Huang J, Rojas M, Vondriska TM, Stefani E, Deb A. Mesenchymal-endothelial transition contributes to cardiac neovascularization. *Nature* 2014;**514**:585–590.
28. Seno A, Kasai T, Ikeda M, Vaidyanath A, Masuda J, Mizutani A, Murakami H, Ishikawa T, Seno M. Characterization of gene expression patterns among artificially developed cancer stem cells using spherical self-organizing map. *Cancer Inform* 2016;**15**:163–178.
29. Lee YS, Hwang SG, Kim JK, Park TH, Kim YR, Myeong HS, Choi JD, Kwon K, Jang CS, Ro YT, Noh YH, Kim SY. Identification of novel therapeutic target genes in acquired lapatinib-resistant breast cancer by integrative meta-analysis. *Tumor Biol* 2016;**37**:2285–2297.
30. Chan HS, Chang SJ, Wang TY, Ko HJ, Lin YC, Lin KT, Chang KM, Chuang YJ. Serine protease PRSS23 is upregulated by estrogen receptor alpha and associated with proliferation of breast cancer cells. *PLoS ONE* 2012;**7**:e30397.
31. LeBleu VS, Teng Y, O'connell JT, Charytan D, Muller GA, Muller CA, Sugimoto H, Kalluri R. Identification of human epididymis protein-4 as a fibroblast-derived mediator of fibrosis. *Nat Med* 2013;**19**:227–231.
32. Teoh JP, Park KM, Broskova Z, Jimenez FR, Bayoumi AS, Archer K, Su H, Johnson J, Weintraub NL, Tang Y, Kim IM. Identification of gene signatures regulated by carvedilol in mouse heart. *Physiol Genomics* 2015;**47**:376–385.
33. Tang Y, Wang Y, Park KM, Hu Q, Teoh JP, Broskova Z, Ranganathan P, Jayakumar C, Li J, Su H, Ramesh G, Kim IM. MicroRNA-150 protects the mouse heart from ischemic injury by regulating cell death. *Cardiovasc Res* 2015;**106**:387–397.
34. Ramakrishna S, Kim IM, Petrovic V, Malin D, Wang IC, Kalin TV, Meliton L, Zhao YY, Ackerson T, Qin Y, Malik AB, Costa RH, Kalinichenko VV. Myocardium defects and ventricular hypoplasia in mice homozygous null for the Forkhead Box M1 transcription factor. *Dev Dyn* 2007;**236**:1000–1013.
35. Kim IM, Ackerson T, Ramakrishna S, Tretiakova M, Wang IC, Kalin TV, Major ML, Gusarova GA, Yoder HM, Costa RH, Kalinichenko VV. The Forkhead Box m1 transcription factor stimulates the proliferation of tumor cells during development of lung cancer. *Cancer Res* 2006;**66**:2153–2161.
36. Fiedler J, Jazbutyte V, Kirchmaier BC, Gupta SK, Lorenzen J, Hartmann D, Galuppo P, Kneitz S, Pena JT, Sohn-Lee C, Loyer X, Soutschek J, Brand T, Tuschl T, Heineke J, Martin U, Schulte-Merker S, Ertl G, Engelhardt S, Bauersachs J, Thum T. MicroRNA-24 regulates vascularity after myocardial infarction. *Circulation* 2011;**124**:720–730.
37. Wang X. miRDB: a microRNA target prediction and functional annotation database with a wiki interface. *RNA* 2008;**14**:1012–1017.
38. Lewis BP, Shih IH, Jones-Rhoades MW, Bartel DP, Burge CB. Prediction of mammalian microRNA targets. *Cell* 2003;**115**:787–798.
39. Krek A, Grun D, Poy MN, Wolf R, Rosenberg L, Epstein EJ, MacMenamin P, da Piedade I, Gunsalus KC, Stoffel M, Rajewsky N. Combinatorial microRNA target predictions. *Nat Genet* 2005;**37**:495–500.

40. Lytle JR, Yario TA, Steitz JA. Target mRNAs are repressed as efficiently by microRNA-binding sites in the 5′ UTR as in the 3′ UTR. *Proc Natl Acad Sci U S A* 2007;**104**:9667–9672.
41. Forman JJ, Legesse-Miller A, Coller HA. A search for conserved sequences in coding regions reveals that the let-7 microRNA targets Dicer within its coding sequence. *Proc Natl Acad Sci U S A* 2008;**105**:14879–14884.
42. Fu Y, Chang AC, Fournier M, Chang L, Niessen K, Karsan A. RUNX3 maintains the mesenchymal phenotype after termination of the Notch signal. *J Biol Chem* 2011;**286**:11803–11813.
43. Ghosh AK, Nagpal V, Covington JW, Michaels MA, Vaughan DE. Molecular basis of cardiac endothelial-to-mesenchymal transition (EndMT): differential expression of microRNAs during EndMT. *Cell Signal* 2012;**24**:1031–1036.
44. Gogiraju R, Xu X, Bochenek ML, Steinbrecher JH, Lehnart SE, Wenzel P, Kessel M, Zeisberg EM, Dobbelstein M, Schafer K. Endothelial p53 deletion improves angiogenesis and prevents cardiac fibrosis and heart failure induced by pressure overload in mice. *J Am Heart Assoc* 2015;**4**:e001770.
45. Feng B, Cao Y, Chen S, Chu X, Chu Y, Chakrabarti S. miR-200b mediates endothelial-to-mesenchymal transition in diabetic cardiomyopathy. *Diabetes* 2016;**65**:768–779.
46. Grisanti LA, Gumpert AM, Traynham CJ, Gorsky JE, Repas AA, Gao E, Carter RL, Yu D, Calvert JW, Garcia AP, Ibanez B, Rabinowitz JE, Koch WJ, Tilley DG. Leukocyte-expressed beta2-adrenergic receptors are essential for survival after acute myocardial injury. *Circulation* 2016;**134**:153–167.
47. Aurora AB, Mahmoud AI, Luo X, Johnson BA, van Rooij E, Matsuzaki S, Humphries KM, Hill JA, Bassel-Duby R, Sadek HA, Olson EN. MicroRNA-214 protects the mouse heart from ischemic injury by controlling Ca(2)(+) overload and cell death. *J Clin Invest* 2012;**122**:1222–1232.
48. Eulalio A, Mano M, Dal Ferro M, Zentilin L, Sinagra G, Zacchigna S, Giacca M. Functional screening identifies miRNAs inducing cardiac regeneration. *Nature* 2012;**492**:376–381.
49. Wang X, Ha T, Zou J, Ren D, Liu L, Zhang X, Kalbfleisch J, Gao X, Williams D, Li C. MicroRNA-125b protects against myocardial ischaemia/reperfusion injury via targetingp53-mediated apoptotic signalling and TRAF6. *Cardiovasc Res* 2014;**102**: 385–395.
50. Xu C, Hu Y, Hou L, Ju J, Li X, Du N, Guan X, Liu Z, Zhang T, Qin W, Shen N, Bilal MU, Lu Y, Zhang Y, Shan H. Beta-blocker carvedilol protects cardiomyocytes against oxidative stress-induced apoptosis by up-regulating miR-133 expression. *J Mol Cell Cardiol* 2014;**75**:111–121.
51. Zhu JN, Chen R, Fu YH, Lin QX, Huang S, Guo LL, Zhang MZ, Deng CY, Zou X, Zhong SL, Yang M, Zhuang J, Yu XY, Shan ZX. Smad3 inactivation and MiR-29b upregulation mediate the effect of carvedilol on attenuating the acute myocardium infarction-induced myocardial fibrosis in rat. *PLoS ONE* 2013;**8**:e75557.
52. Matkovich SJ, Wang W, Tu Y, Eschenbacher WH, Dorn LE, Condorelli G, Diwan A, Nerbonne JM, Dorn GW 2nd. MicroRNA-133a protects against myocardial fibrosis and modulates electrical repolarization without affecting hypertrophy in pressure-overloaded adult hearts. *Circ Res* 2010;**106**:166–175.
53. Castaldi A, Zaglia T, Di Mauro V, Carullo P, Viggiani G, Borile G, Di Stefano B, Schiattarella GG, Gualazzi MG, Elia L, Stirparo GG, Colorito ML, Pironti G, Kunderfranco P, Esposito G, Bang ML, Mongillo M, Condorelli G, Catalucci D. MicroRNA-133 modulates the beta1-adrenergic receptor transduction cascade. *Circ Res* 2014;**115**:273–283.
54. Zhang Y, Huang XR, Wei LH, Chung AC, Yu CM, Lan HY. miR-29b as a therapeutic agent for angiotensin II-induced cardiac fibrosis by targeting TGF-beta/Smad3 signaling. *Mol Ther* 2014;**22**:974–985.
55. Wahlberg P, Nylander A, Ahlskog N, Liu K, Ny T. Expression and localization of the serine proteases high-temperature requirement factor A1, serine protease 23, and serine protease 35 in the mouse ovary. *Endocrinology* 2008;**149**:5070–5077.